INVESTIGATION ON 3D PRINTED MICROWAVE LENS FOR HORN ANTENNA

Goh Wei En[1], Yee Yi Xin Kristen[1], Ang Teng Wah[2], Lim Zi Wei[2], Huang Yingying[2]
[1] CHIJ St. Nicholas Girls' School, Ang Mo Kio Street 13, Singapore 569405
[2]DSO National Laboratories, 12 Science Park Drive, Singapore 118225

Abstract

In this paper, an investigation on the use of a microwave Polylactic Acid (PLA) lens of homogeneous dielectric constant with a horn antenna to achieve a flat top beam with high roll off and low sidelobes at X-band is presented. The lens is made of 6 concentric rings of height ranging from 8-16mm. The lens and antenna was simulated with Ansys HFSS, 3D printed with PLA and then measured in an anechoic chamber at 8-12GHz. Simulation and measurement data are presented and discussed. The measured lens achieved a peak gain of 10.9dBi and 3dB beamwidth of 54 degrees. In conclusion, a microwave lens that can alter the radiation pattern of a horn antenna of 12.2dBi peak gain and 3dB beamwidth of 42 degrees to give a flat top beam with steep roll off and low sidelobes was achieved.

1. Introduction

A flat top beam is characterised by a radiation pattern with a constant gain and a flat intensity profile over a certain range of angles. It has many applications including wireless communications [1-2] and search RADARs [3], where a constant field in a specific direction is needed.

When measuring and testing antenna performance in an anechoic chamber, signals from the transmitting antenna may be reflected by objects inside and cause distortions in the measured radiation pattern. To combat this issue, a flat top beam with low sidelobes, which provides constant flux illumination within a specific range, can be used. The steep roll off and low sidelobe levels of a flat top beam aid in directing energy to the desired direction, thus minimising interference from other objects.

3D printing is an additive manufacturing technology that can manufacture complex objects with low cost and reduced production time [4]. This process enables the creation of air spaces in the lens not achievable by traditional machining [5], thus resulting in a wider range of dielectric constants.

Methods of achieving a flat top beam such as using antenna arrays [2, 3, 6] or Gradient Index lenses [7] have been studied. One such method is by using a microwave lens with a horn antenna. Therefore, in this paper, we investigate the use of 3D printing to construct a microwave lens capable of creating a flat top radiation pattern with a horn antenna.

2. Materials and Methods

2.1 Simulation

The horn antenna and microwave lens were modelled in the Ansys Electronics Desktop Student 2023 R2 software. All simulations were solved at a frequency of 10GHz and in the H plane. The simulation setup is shown in Fig. 1.

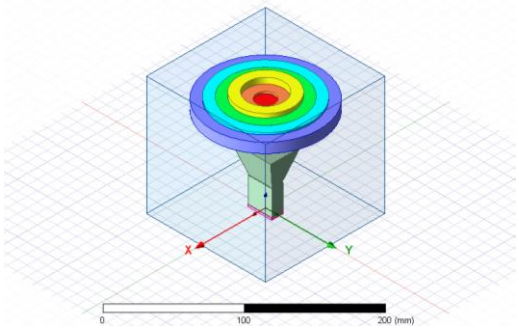

Fig. 1 Simulation setup of horn antenna and microwave lens inside airbox in Ansys simulator

2.1a Horn antenna

The designed horn antenna consists of a WR90 waveguide feed and a flare section for radiation. The horn antenna was designed by varying the dimension of the aperture and flare length to obtain a minimum peak gain of 8.5dBi and 3dB beamwidth of about 45 degrees. The simulated flare that achieved the closest match for 3dB beamwidth was then 3D printed and measured.

2.1b Microwave lens

The microwave lens is circular with 6 concentric rings of homogenous PLA material of the same infill density. The diameter of the lens is 108mm to cover the entire aperture of the horn antenna.

The variables varied in the simulation were the dielectric constant of the lens, distance between the lens and the antenna, and the height of each ring. The height of each ring was varied from 8-20mm in increments of 2mm, while the distance was varied from 0-100mm. The lens that produced the most optimal radiation pattern was then 3D printed and measured.

2.2 3D printing and measurements

The microwave lens and antenna flare were printed using a Cubicon Style 3D printer. The antenna flare in Fig. 2 was printed with PLA+ and lined with copper tape to metallise the walls. The lens in Fig. 3 was printed with PLA+ with a triangular infill at 66% density. The dielectric constant of the lens was taken to be 2.1277 [8]. Additionally, the same lens design was printed but with the top and bottom 0.6mm sections printed with 100% infill density and is shown in Fig. 4. The far-field measurements of the antenna and lens were measured in an anechoic chamber at 8-12 GHz.

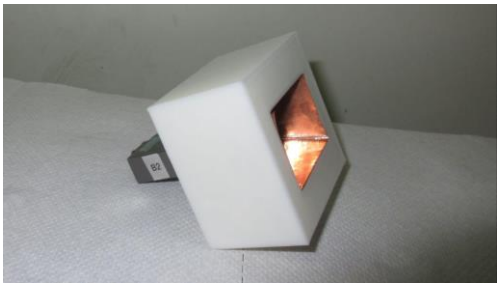

Fig. 2 3D printed antenna flare and WR90 waveguide

Fig. 3 Picture and close up of 3D printed microwave lens with triangular infill at 66% density

Fig. 4 Picture and close up of 3D printed microwave lens with triangular infill at 66% density and 0.6mm top and bottom sections of 100% infill density

2.3 Performance indicators

The performance indicators used to evaluate the performance of the microwave lens are listed in Table 1, along with the definitions and goal of each indicator. Some indicators are depicted in Fig. 5. Flatness, roll off, and gain of the first sidelobe were prioritised.

Table 1 Definitions and goal of performance indicators

Indicator	Definition	Goal
Span	Range in which we want to achieve a flat top	45 degrees
Flatness	Difference between the maximum and minimum points within the span	Lower
Roll off	Absolute value of gradient between edge of span and next minimum point	Higher
Gain of first sidelobe	Gain of first maximum turning point outside of the span	Lower
Angle of first sidelobe	Angle of first maximum turning point outside of the span	Larger
Gain of far-out sidelobes	Gain of subsequent sidelobes beyond the span	Lower

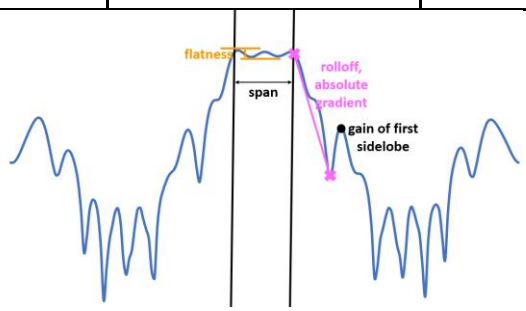

Fig. 5 Diagram of performance indicators

3. Results

3.1 Horn antenna

3.1a Simulated antenna

The final flare in Fig. 6 had an aperture of 30mmx40mm with a flare length of 30mm. The simulated antenna achieved a peak gain of 12.2dBi peak gain, with a 3dB beamwidth of 42 degrees, as shown in Fig. 7.

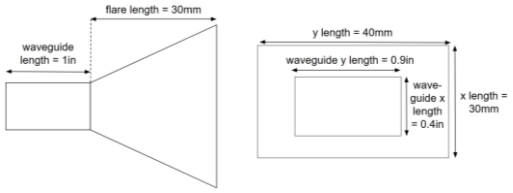

Fig. 6 Diagram of horn antenna

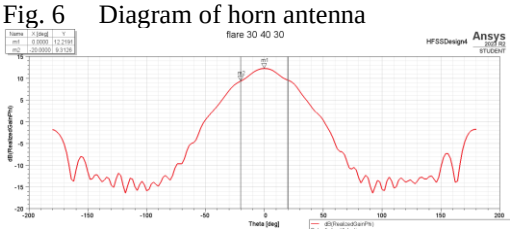

Fig. 7 Radiation pattern of the simulated horn antenna

3.1b 3D printed antenna

The radiation pattern of the 3D printed antenna resulted in a lower gain than in simulation, as shown in Fig. 8. However, the 3dB beamwidth and shape of the 3D printed flare are similar to that of the simulated flare.

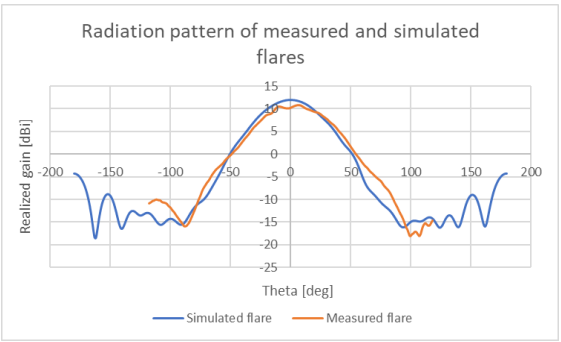

Fig. 8 Comparison of the simulated and measured radiation patterns of the horn antenna

3.2 Microwave lens

3.2a Simulated lens

Various simulated lenses were evaluated based on performance indicators described in Section 2.3. Lenses with unfavourable characteristics were eliminated. The remaining lenses were compared on flatness, roll off and gain of first sidelobes as shown in Fig. 9 and 10.

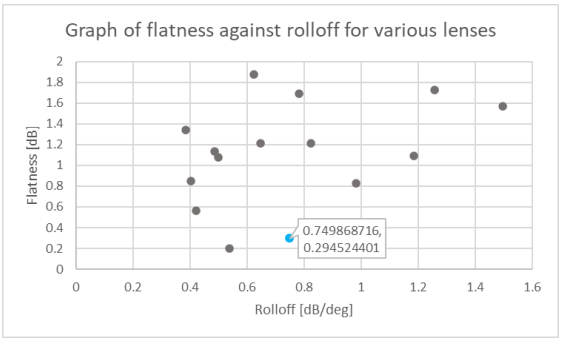

Fig. 9 Scatter plot of flatness against rolloff for each microwave lens

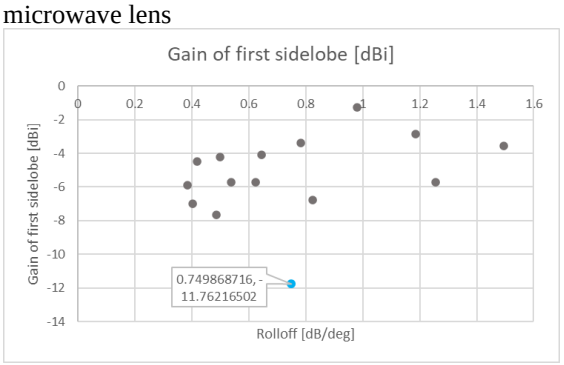

Fig. 10 Scatter plot of gain of first sidelobe against roll off for each microwave lens

The simulated performance of the chosen lens had a flatness of 0.29dB, roll off of 0.75dB/degrees and sidelobe levels of -11.8dBi. It had the lowest first sidelobe levels and was second best in terms of flatness. The heights and radii of each ring are shown in Fig. 11. The optimal performance was achieved at 30mm, and the radiation pattern is shown in Fig. 12.

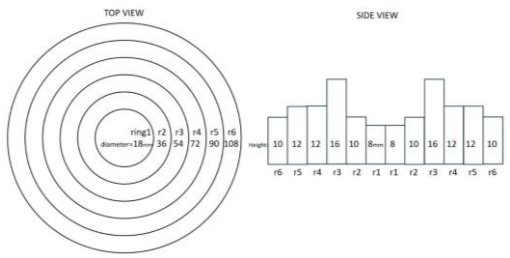

Fig. 11 Top and side views of the final microwave lens

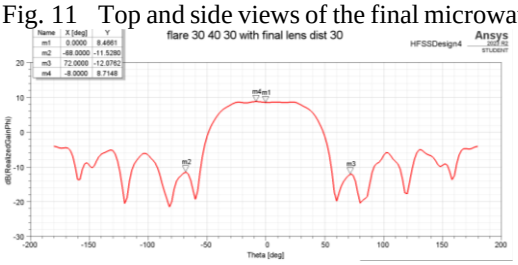

Fig. 12 Radiation pattern of the final lens at 30mm away from the antenna

3.2b 3D printed lens

The 3D printed lens was measured with the setup shown in Fig. 13 and the radiation pattern was plotted with averaging. The radiation pattern of the simulated and measured flares have good agreement, with similar shapes, gains and roll offs, as seen in Fig. 14.

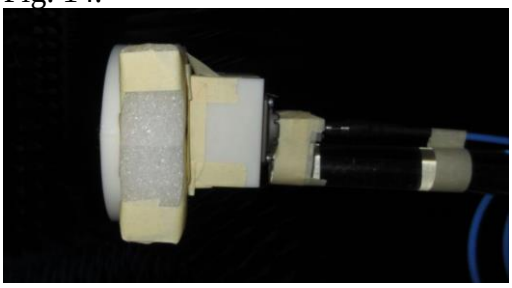

Fig. 13 Side view of setup of antenna and lens at 30mm distance apart

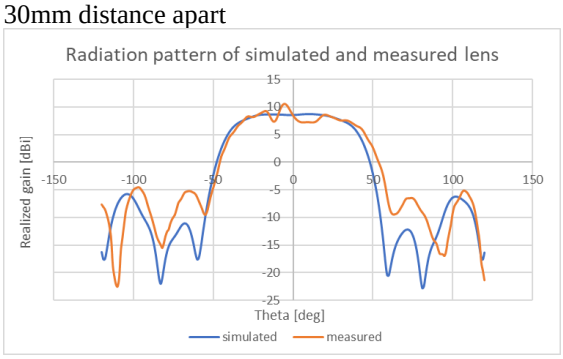

Fig. 14 Comparison of the simulated and measured radiation patterns of the final lens at 30 mm distance

However, an abnormal kink is present in the radiation pattern at theta=-16 to -5 degrees, causing the radiation pattern to be unsymmetrical. This could be due to measurement errors or tolerances incurred in the fabrication of the lens.

3.3 Simulated variables and trends

In the simulator, the effect of varying distance and dielectric constant were investigated for 3 different lens profiles: flat, converging and diverging, which are shown in Fig. 15, 16 and 17.

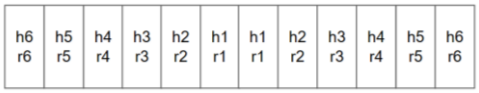

Fig. 15 Side view of lens with flat profile

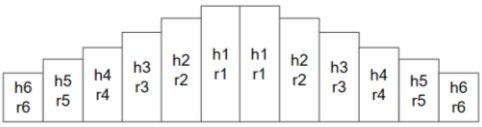

Fig. 16 Side view of lens with converging profile

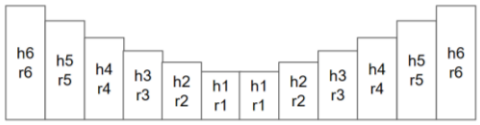

Fig. 17 Side view of lens with diverging profile

The heights used for each lens profile when varying distance and dielectric constant are listed in Table 2.

Table 2 Heights of each lens profile when varying dielectric constant and distance

Lens profile	**h1/ mm**	**h2/ mm**	**h3/ mm**	**h4/ mm**	**h5/ mm**	**h6/ mm**
Flat	10	10	10	10	10	10
	20	20	20	20	20	20
	40	40	40	40	40	40
Converging	8	7	6	5	4	3
Diverging	3	4	5	6	7	8

3.3a Distance between microwave lens and horn antenna

For the converging lens profile, increasing distance generally resulted in increased peak gain, higher sidelobes and a narrower 3dB beamwidth, as seen in Fig. 18.

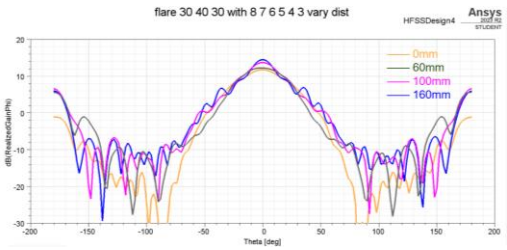

Fig. 18 Radiation patterns of converging lens at various distances away from horn antenna

For a diverging or flat lens profile, increasing the distance results in decreased gain. The peak reduces, forming either a null or a flat top. A further increase in distance causes the peak to increase, the 3dB beamwidth to narrow and the gain of the sidelobes to increase, as shown in Fig. 19 and 20.

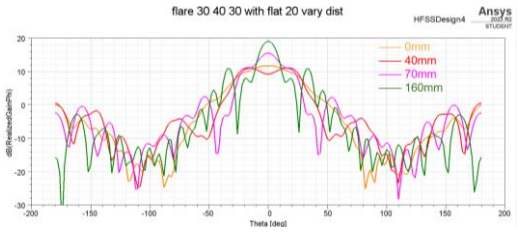

Fig. 19 Radiation patterns of flat 20 mm lens at various distances away from horn antenna

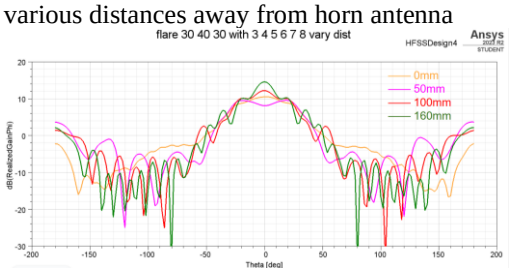

Fig. 20 Radiation patterns of diverging lens at various distances away from horn antenna

As shown in Fig. 21, varying the distance for our chosen lens resulted in a similar trend as the diverging and flat lenses. As the distance increases, the gain decreases, forming a null. The 3dB beamwidth also increases. Afterwards, the gain increases, producing a flat top before forming a higher peak. The 3dB beamwidth also decreases.

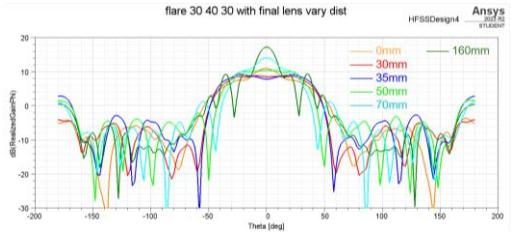

Fig. 21 Radiation patterns of chosen lens at various distances away from horn antenna

After a certain point, distance has little effect on lens performance. The 3dB beamwidth becomes constant and all lenses have similar radiation patterns regardless of the profile. This could indicate that the lens is ineffective at a large distance as the angle subtended to the lens is small thus it receives little illumination from the antenna.

Additionally, when comparing the trend in 3dB beamwidth for flat lenses of different thicknesses, the graph for the 40mm thick flat lens plateaued at a smaller distance as seen in Fig. 22. Thus, a change in distance could be more significant for a thicker lens.

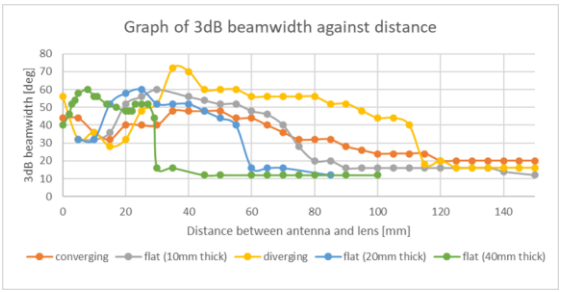

Fig. 22 Graph of 3dB beamwidth against distance for various lens profiles

As shown in Fig. 23, there are optimal points to obtain a flat top beam for all the lenses shown. Graphs for the diverging and flat lenses appear to have multiple optimal points, but not the converging lens.

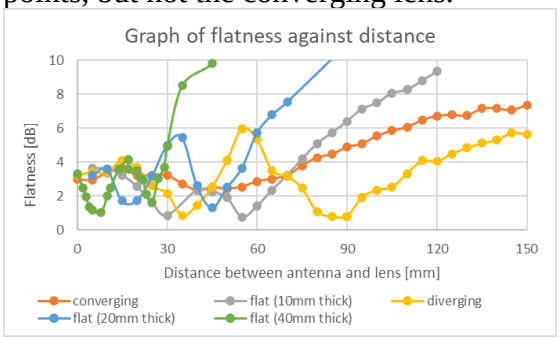

Fig. 23 Graph of flatness against distance between for various lens profiles

3.3b Dielectric constant of microwave lens

For a converging lens profile, varying the dielectric constant resulted in increased peak gain and narrowed 3dB beamwidth overall, as shown in Fig. 24.

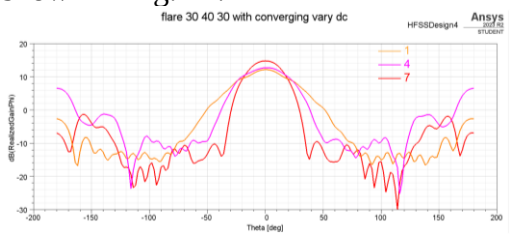

Fig. 24 Radiation patterns of a converging lens with various dielectric constants

For the diverging lens profile, an increase in dielectric constant caused the gain at theta=0 degrees to decrease, the 3dB beamwidth to narrow and the gain of the sidelobes to increase. The peak reduces and flattens. A further increase in dielectric constant resulted in higher gain at theta=0 degrees while the 3dB beamwidth narrowed and the gain of sidelobes increased. Ripples

were observed in the main lobe and became more pronounced. This can be seen in Fig. 25.

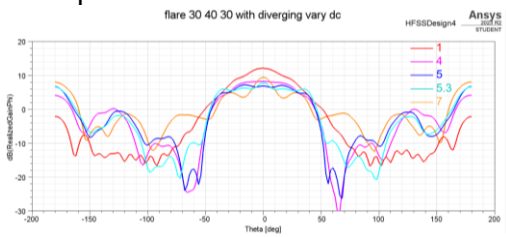

Fig. 25 Radiation patterns of a diverging lens with various dielectric constants

For a flat lens, an increase in dielectric constant resulted in narrower 3dB beamwidth, lower gain at theta=0 degrees and increased gain of sidelobes. The peak reduces and flattens. A further increase in dielectric constant resulted in the gain at theta=0 degrees to decrease further, forming a null. This can be seen in Fig. 26.

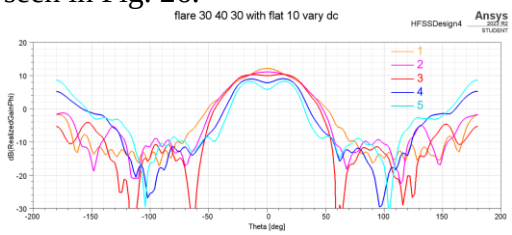

Fig. 26 Radiation patterns of a flat lens of 10 mm with various dielectric constants

For the diverging, flat and final lenses, there is an optimal point where a flat top can be achieved with a flatness of less than 2dB as shown in Fig. 27. However, for the converging lens, the flatness appears to remain above the 2dB mark, and it is not very flat at these dielectric constants.

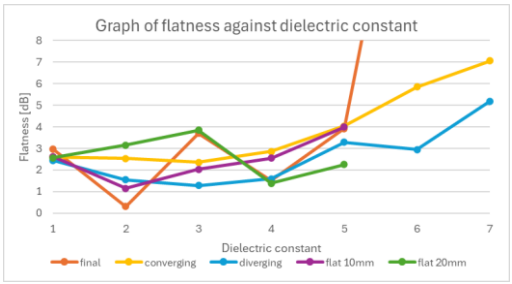

Fig. 27 Graph of flatness against dielectric constant for various lenses profiles

Within the range of dielectric constants for PLA, which is taken to be 1.7778 to 2.8141 [8], the dielectric constant had minimal effect. The largest change was observed when the lens was thickest, as shown in Fig. 28. Therefore, it appears that for a thinner lens, to achieve a similar radiation pattern as a thicker lens, the dielectric constant has to be further increased.

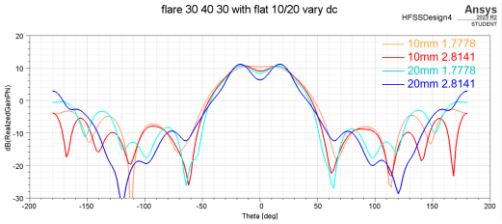

Fig. 28 Radiation patterns of 2 flat lenses (10mm and 20mm) with dielectric constants of 1.7778 and 2.8141

3.3c Curvature of microwave lens

To increase the curvature of the lens, the step size (p) was varied from 0.5mm to 9mm in increments of 0.5mm. The heights of each ring are listed in Table 3.

Table 3 Heights of each ring of microwave lens when varying curvature of lens

Lens profile	h1/ mm	h2/ mm	h3/ mm	h4/ mm	h5/ mm	h6/ mm
Conve-rging	1+5 p	1+4 p	1+3p	1+2p	1+p	1
Diverg-ing	1	1+p	1+2p	1+3p	1+4p	1+5p

For the converging lens, as the step size increases, the peak gain increases while the 3dB beamwidth narrows. The gain of the first sidelobe also increases, as seen in Fig. 29.

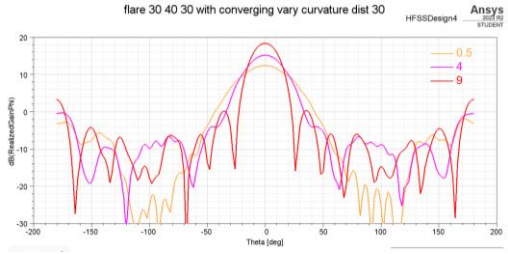

Fig. 29 Radiation pattern of converging lens with various step sizes

For the diverging lens, as the curvature increases, the peak gain decreases and 3dB beamwidth widens. The peak reduces and flattens. However, as the step size increases past 3mm, the peak gain increases, the 3dB beamwidth narrows and the gain of sidelobes increases. A mainlobe with 3 peaks is also observed. Further increase in curvature causes

the nulls of the main lobe to deepen. The first sidelobes decrease while the far-out sidelobes increase as seen in Fig. 30.

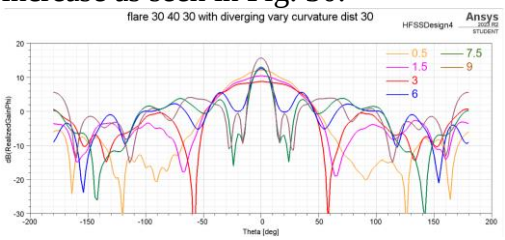

Fig. 30 Radiation pattern of diverging lens with various step sizes

3.4 3D printed lens and trends

3.4a Distance between microwave lens and horn antenna

When increasing the distance between the 3D printed lens and antenna, the gain at theta=0 degrees generally increases as shown in Fig. 31. The 3dB beamwidth widens then narrows as shown in Fig. 32. This is similar to the trends that were observed in the simulation.

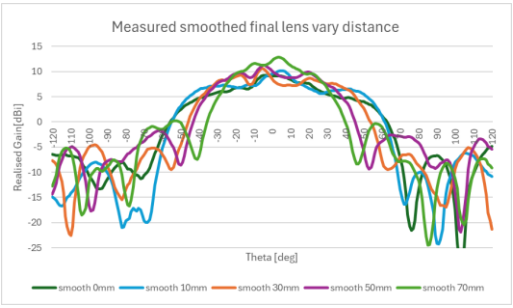

Fig. 31 Radiation pattern of measured lens with varying distance at 10GHz

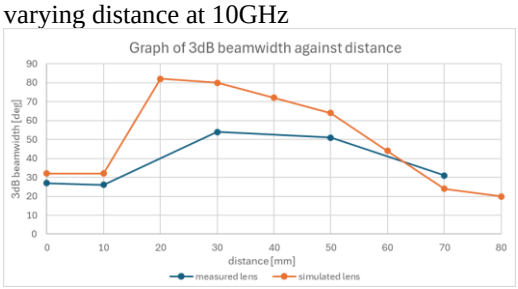

Fig. 32 Comparison of 3dB beamwidth against distance of measured lens and simulated lens

3.4b Dielectric constant of microwave lens

The first lens was printed with 66% infill and had a dielectric constant of 2.1277 [8]. The second lens was printed with 66% infill with the top and bottom 0.6mm sections being of 100% infill. Both lenses are shown in Fig. 33.

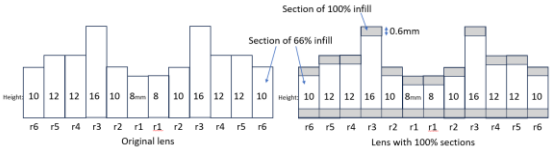

Fig. 33 Comparison of side view of original lens and lens with 100% infill sections

As shown in Fig. 34, the radiation patterns were very similar, however, the abnormal kink was more pronounced for the lens with additional layers.

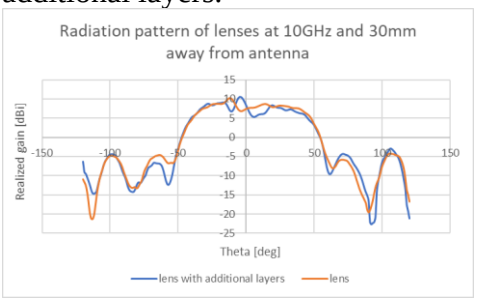

Fig. 34 Radiation patterns of both 3D printed lenses at 30mm distance at 10GHz

3.4c Frequency

Generally for all distances, as frequency increases, the gain increases and the beam becomes narrower. The comparison of different frequencies at 30mm is shown in Fig. 35. This could be due to the narrowed 3dB beamwidth and higher gain of the horn radiation pattern as frequency increases, as shown in Fig. 36.

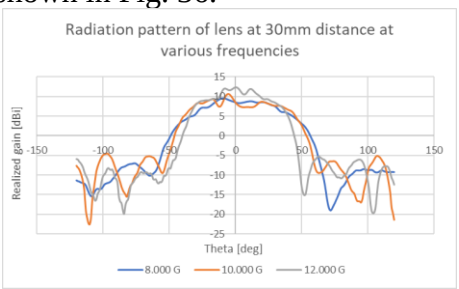

Fig. 35 Radiation patterns of chosen lens at 30mm distance at various frequencies

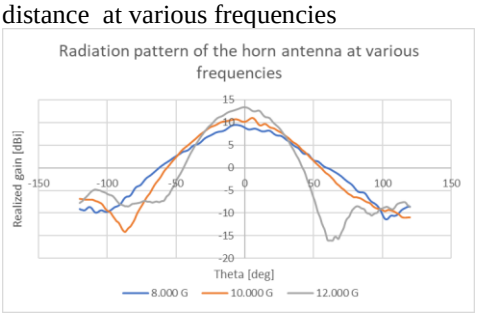

Fig. 36 Radiation pattern of horn antenna at various frequencies

As frequency increases, the difference between the maximum and minimum within the span increases. From 8-10GHz, the difference ranges from 0.883-3.39dB. The difference peaks at 10.2GHz and decreases, becoming more flat as the frequency increases further, as shown in Fig. 37.

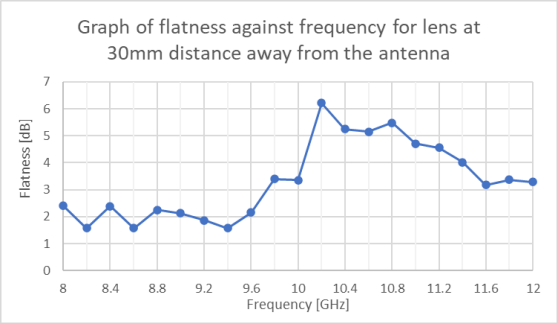

Fig. 37 Graph of flatness against frequency of chosen lens at 30mm distance

However, the large abnormal kink was present in the measured radiation pattern from 9.8-12.0GHz, which affects the flatness reading, as the difference between the max and min within the span will be exaggerated. The increase and subsequent decrease in the size of the kink could be responsible for the increase then decrease in flatness.

A better indicator might be simply taking the flatness from theta > 0, as the kink is roughly around -16 to -5 degrees. As seen in Fig. 38, the patterns become less flat as the frequency increases.

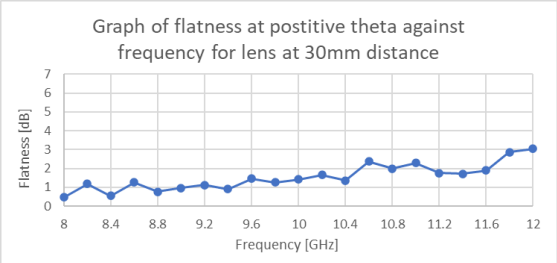

Fig. 38 Graph of flatness at positive theta against frequency for chosen lens at 30mm distance

4. Discussion

4.1 General observations

In simulation, the heights of the 6 rings, distance and dielectric constant were varied. However, as it is time-consuming to simulate such a large number of lenses, both the distance and dielectric constants can be fixed and the heights varied. The distances or dielectric constants of lenses that produce flat radiation patterns can then be varied to achieve even better performance.

Additionally, it is worth noting that after a certain point, increasing the distance does not result in changes in the radiation pattern. Thus, there is no reason to simulate past that particular distance. For a thicker lens, that distance is shorter. If one is simulating for a thicker lens, the distance need not be varied as much as for a thinner lens.

It was also found that some microwave lenses (with diverging and flat profiles) could have multiple distances and dielectric constants in which a flat top beam would be produced. However, the 3dB beamwidth, rolloff and gain of the sidelobes are different for each distance. This may allow a single microwave lens to meet different requirements when placed at different distances from the horn antenna.

Lastly, 3D printing was found to be a feasible method for rapid prototyping of microwave lenses as the lens can be created quickly and saves time. It is also effective at creating a lens that can alter the radiation pattern of an antenna.

4.2 Limitations and further research

When measuring the radiation pattern of the lens, an abnormal kink was found. Due to a lack of time, the cause of this kink was not investigated. To mitigate this problem, it is preferable to use a ready-made horn antenna for both simulation and measurement.

Furthermore, exploring alternative shapes such as rectangles may lead to radiation patterns that are more optimal. By varying parameters such as the dimensions of the lens and the dielectric constant of different rings, the radiation pattern may be further optimised. Different materials such as Acrylonitrile-Butadiene-Styrene (ABS) could also be explored.

5. Conclusion

After simulating and measuring the radiation patterns of the microwave lens and horn antenna, we can conclude that the microwave lens is effective in altering the radiation pattern of a horn antenna and that a

flat top beam with steep roll off and low sidelobes can be achieved. The microwave lens and horn antenna was simulated and 3D printed, then measured in an anechoic chamber. The measured radiation patterns are similar to the simulated ones, which shows that the use of 3D printing is effective to achieve our desired radiation pattern.

Acknowledgements

We would like to express our deep gratitude to our mentors, Dr Ang Teng Wah, Ms Huang Yingying and Mr Lim Zi Wei for their invaluable guidance throughout this project. We would also like to thank Ms Joyce Yao for their support.

References

[1] Zhang, Z., Liu, N., Zuo, S., Li, Y., Fu, G. 2015. Wideband circularly polarised array antenna with flat-top beam pattern. IET Microwaves, Antennas & Propagation, Vol. 9, No. 8: 755-761

[2] Milijić, M. R., Nešić, A. D., Milovanović, B. D., Nešić, D. A. 2017. Printed Antenna Array with Flat-Top Radiation Pattern. Frequenz, Vol. 72, No. 5-6: 173-180

[3] Angeletti, P., Buttazzoni, G., Toso, G., Vescovo, R. 2021. Parametric Analysis of Linear Periodic Arrays Generating Flat-Top Beams. Electronics, Vol. 10, No. 20; Microwave and Wireless Communications; High-Performance Antenna Design and Applications

[4] Munina, I., Grigoriev, I., O'Donnell, G., Trimble, D. 2023. A Review of 3D Printed Gradient Refractive Index Lens Antennas. IEEE Access Volume 11: 8790-8809

[5] Zhang, S., Arya, R. K., Pandey, S., Vardaxoglou, Y., Whittow, W., Mittra, R. 2016. 3D-Printed Planar Graded Index Lens. IET Microwaves, Antennas & Propagation Volume 10 Issue 13: 1411-1419

[6] Xu, M., Zhang, C., Qiao, H., Zhang, Q., Deng, C., Yu, W. 2023. Sparse Antenna Array With Flat-Top and Sharp Cutoff Radiation Patterns. IEEE Transactions on Antennas and Propagation, Vol. 71, No. 6: 4695-4703

[7] Yin, S., Li, J., Ye, Q., Zhang Y. 2023. Low-profile metasurface lens antenna with flat-top radiation pattern. International Journal of Electronics and Communications, Vol. 170, Article 154819

[8] Kuzmanic, I., Vujovic, I., Petkovic, M. and Josko, S. 2023. Influence of 3D printing properties on relative dielectric constant in PLA and ABS materials. Progress in Additive Manufacturing, Vol. 8: 703-710